

1  
2  
3  
4  
5  
6 Planar diffusion to macro disc electrodes - What electrode size is required for  
7 the Cottrell and Randles-Sevcik equations to apply quantitatively?<sup>†</sup>  
8  
9

10  
11 Kamonwad Ngamchuea, Shaltiel Eloul, Kristina Tschulik, Richard G Compton\*

12  
13  
14  
15  
16 Department of Chemistry, Physical & Theoretical Chemistry Laboratory, Oxford University, South Parks  
17 Road, Oxford, OX1 3QZ, United Kingdom  
18  
19

20  
21  
22 \*corresponding author: Richard G. Compton, PTCL, Department of Chemistry, University of Oxford,  
23 South Parks Road, Oxford, OX1 3BW, U.K.  
24

25  
26 Email: [richard.compton@chem.ox.ac.uk](mailto:richard.compton@chem.ox.ac.uk). Tel: +44 (0) 1865 275 957 Fax: +44 (0) 1865 275410  
27  
28  
29

30 **Key Words:**  
31

32  
33 Mass transport, one-dimensional planar diffusion, Cottrell equation, Randles-Sevcik equation,  
34 chronoamperometry, cyclic voltammetry  
35  
36  
37  
38  
39

40 **Abstract**  
41

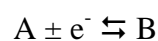
42  
43 Simulations and experiments are reported which investigate the size of a macro disc electrode necessary to  
44 *quantitatively* show the chronoamperometric or voltammetric behaviour predicted by the Cottrell equation  
45 or the Randles-Sevcik equation on the basis of exclusive one-dimensional diffusional mass transport. For  
46 experimental time scales of several seconds, the contribution of radial diffusion is seen to be measurable  
47 even for electrodes of millimetres in radius. Recommendations on the size of macro electrodes for  
48 quantitative study are given and should exceed 4 mm radius in aqueous solution.  
49  
50  
51  
52  
53  
54  
55  
56

57 **Introduction**  
58

59  
60 <sup>†</sup> Paper submitted for the 'Fletcher Festschrift' issue of Journal of Solid State Electrochemistry in admiration of an outstanding  
61 scientist and much valued electrochemistry colleague.  
62  
63  
64  
65

1  
2  
3 The use of microelectrodes for the best-practice measurement of electrochemically derived data, such as  
4 heterogeneous rate constants, diffusion coefficients, fast coupled homogeneous reaction kinetics and  
5 analytical considerations, is well-established. This approach is largely based on the pioneering work of  
6 Amatore [1, 2] and was further implemented by Bond [3, 4] and others [5, 6]. Recently – and partly  
7 driven by the need to interrogate the diverse, complex and ever increasingly imaginative methods for  
8 possible energy conversion and storage as well as for analysis – there has been a renaissance in macro  
9 electrode measurements both employing rotating disc electrodes [7, 8], but also, and especially, cyclic  
10 voltammetry using macro electrodes [9], as originally introduced by the classical work of Nicholson and  
11 Shain [10, 11].

12  
13  
14 The simplicity of using macro electrodes, other than the practical ease of size, lies in the assumption that  
15 diffusional transport to the electrode surface will be planar and one-dimensional. Thus, and usually in  
16 contrast to microelectrodes, theoretical equations can often be derived in mathematically analytical forms  
17 for the purpose of comparison with experiments. Thus, the current-time ( $I-t$ ) response resulting from a  
18 potential step from zero current to diffusion-limited conditions applied to the sample redox process:



30  
31  
32 is given by the Cottrell equation known to all electrochemists [12]:

$$33 \quad I = \frac{FA\sqrt{D}}{\sqrt{\pi t}} [A]_{\text{bulk}} \quad (1)$$

34  
35 where  $D$  is the diffusion coefficient,  $[A]_{\text{bulk}}$  the bulk concentration of species A in the solution,  $F$  is the  
36 Faraday constant and  $A$  the electrode area (for a disc of radius  $r_e$  the area  $A = \pi r_e^2$ ).

37  
38 Similarly, assuming that the redox couple A/B is electrochemically reversible under the prevailing mass  
39 transport conditions, the peak current  $I_p$  for cyclic voltammetry is predicted to be:

$$40 \quad I_p = 0.446 F \pi r_e^2 \sqrt{\frac{FD\nu}{RT}} [A]_{\text{bulk}} \quad (2)$$

41  
42 where  $\nu$  is the scan rate,  $T$  is the temperature and  $R$  the universal gas constant[13]. Both equations (1) and  
43 (2) result from solving Fick's laws of diffusion [14, 15] in one spatial dimension with the appropriate  
44 boundary conditions.

45  
46 Given the renaissance of macro electrode measurements, it is interesting to consider under which  
47 conditions equations (1) and (2) can be applied *quantitatively*, not least since it has recently been asserted

1  
2  
3 that macro electrode experiments may lead to a great diversity of results when applied to the same system,  
4 but by different groups [16–18]. Moreover, this variation has been such as to apparently stimulate the  
5 introduction of elaborate new techniques such as FFT (Fast Fourier Transformation) voltammetry in an  
6 attempt to improve the reproducibility [19, 20].  
7  
8  
9

10  
11 Among the primary features for the applicability of equation (1) and (2) are the need for tight  
12 thermostating, application of the appropriate potential range such that the voltage seen is not reversed  
13 prematurely relative to a cyclic voltammetry peak [13], the avoidance of using second or later scan data,  
14 the avoidance of natural convection [21, 22] the recognition that the use of a digital potentiostat can  
15 broaden voltammetric measurements [23] and the need to ensure that the electrode is flat and neither  
16 rough nor porous [24, 25]. However, one further very simple consideration has to be addressed, namely  
17 how large does the electrode have to be in order to quantitatively comply with equations (1) and (2)? In  
18 other words what is the contribution of radial diffusion (often referred to as ‘edge effect’) to  
19 chronoamperometry and cyclic voltammetry carried out at macro electrodes? Answering these questions is  
20 the aim of this present note and will be approached from both simulation and experimental perspectives.  
21  
22  
23  
24  
25  
26  
27  
28  
29  
30  
31  
32

## 33 **Experimental**

### 34 Chemicals and electrochemical setup

35  
36 The electrolyte used was an aqueous solution of 9.50 mM of potassium ferrocyanide  $K_4[Fe(CN)_6]$   
37 (Lancaster, UK) and 0.50 M potassium nitrate  $KNO_3$  (BDH). This solution was prepared by dissolving the  
38 respective analytical grade chemicals in high-purity water (Millipore, resistivity not less than 18.2 M $\Omega$ cm  
39 at 25 °C).  
40  
41  
42  
43  
44  
45

46 Electrochemical measurements were performed using a three electrode setup comprising a carbon rod  
47 counter electrode, a saturated calomel reference electrode (SCE,  $E = 0.241$  V vs standard hydrogen  
48 electrode, BASi Inc.) and either one of two differently sized glassy carbon working electrodes (BASi  
49 Inc.). The two working electrodes were sized to  $1.49 \pm 0.02$  mm and  $0.78 \pm 0.03$  mm in radius using optical  
50 microscopy (Unicam Instruments LTD). The working electrodes were first polished to a mirror surface  
51 using diamond spray (Kemet, particle size 1.0  $\mu$ m and 0.3  $\mu$ m) and then sonicated in high-purity water for  
52 1 minute prior to each measurement. During electrochemical measurements tight thermostating of the  
53 entire electrochemical cell to under  $\pm 0.2$  °C was ensured by placing the cell in a thermostated water bath  
54  
55  
56  
57  
58  
59  
60  
61  
62  
63  
64  
65

1  
2  
3 inside a thermostated Faraday cage. All measurements were performed in stagnant solutions using a  
4  $\mu$ Autolab III (Metrohm) potentiostat.  
5  
6  
7  
8  
9

### 10 Diffusion coefficient measurements

11  
12  
13 Temperature-dependent diffusion coefficients of  $[\text{Fe}(\text{CN})_6]^{4-}$  in the used electrolyte were determined by  
14 steady-state voltammetry at a platinum micro disc working electrode (radius = 4.8  $\mu\text{m}$ , calibrated using  
15 ruthenium hexa-amine) in the temperature range from 24.0  $^\circ\text{C}$  to 28.0 $^\circ\text{C}$ . The potential was scanned from  
16 -0.15 V to 0.6 V vs SCE at a scan rate of 25  $\text{mVs}^{-1}$ .  
17  
18  
19  
20

### 21 Chronoamperometry

22  
23  
24 To quantify the effect of radial diffusion on chronoamperometry at conventional commercial ‘macro’  
25 electrodes the oxidation of ferrocyanide at two differently sized glassy carbon electrodes was studied  
26 under mass transport limited conditions. For this purpose, the applied potential was changed from -0.2 V  
27 vs SCE to 0.35 V vs. SCE in a single step and the resulting current was recorded for 10 seconds. For each  
28 electrode size three separate chronoamperometric experiments were performed. Blank measurements were  
29 acquired in a solution of 0.50 M  $\text{KNO}_3$  and were subtracted from the chronoamperograms obtained in the  
30 presence of ferrocyanide to remove capacitive contributions from the Faradaic signal.  
31  
32  
33  
34  
35  
36

37 Convection of the electrolyte was kept at an experimental minimum by avoiding temperature gradients  
38 and mechanical perturbation of the electrolyte as well as by restricting the experimental time scale to short  
39 durations (10 s) in order to avoid natural convection.  
40  
41  
42  
43

### 44 Simulation

45  
46 A simulation for a cyclic voltammetry measurement was carried out for an ideal reduction/oxidation  
47 system containing a disc electrode with varied radius. In the model the transport of the electrochemical  
48 species in solution is described for fully supported electrolyte conditions. The thus obtained diffusion  
49 controlled system was solved numerically using Fick's second law in a two-dimensional cylindrical space  
50 [26]:  
51  
52  
53  
54

$$55 \frac{\partial[A]}{\partial t} = D \left( \frac{\partial^2[A]}{\partial r^2} + \frac{1}{r} \frac{\partial[A]}{\partial r} + \frac{\partial^2[A]}{\partial z^2} \right) \quad (3)$$

56  
57  
58  
59  
60  
61  
62  
63  
64  
65

1  
2  
3 for a representative  $D$  of  $10^{-9} \text{ m}^2\text{s}^{-1}$  and an initial concentration of  $[A] = 1 \text{ mM}$ . A reversible boundary  
4  
5 condition was applied on the disc electrode surface to relate the potential  $V$  to the surface concentrations  
6  
7 of the oxidant  $c_{\text{ox}}$  and the reductant  $c_{\text{red}}$  were described by the Nernst expression:

$$(V - E_f^\ominus) \frac{F}{RT} = \ln \left( \frac{c_{\text{ox}}}{c_{\text{red}}} \right) \quad (4)$$

8  
9  
10  
11  
12  $E_f^\ominus$  is the formal potential. Insulation boundary conditions are used for the cell walls and axial symmetry  
13  
14 condition at  $r = 0$ . We also simulated a ‘macro’ case of an infinite disc radius using a one dimensional  
15  
16 system. In this case the Fick's second law follows:

$$\frac{\partial[A]}{\partial t} = D \left( \frac{\partial^2[A]}{\partial x^2} \right) \quad (5)$$

17  
18  
19  
20  
21  
22  
23 The simulations of the cyclic voltammetry were made using a finite difference approach based on the  
24  
25 Alternating Direction Implicit (ADI) method as detailed fully in ref [27]. The simulations were coded in  
26  
27 C++ with the Open Multi-Processing (OpenMP) library for parallel computing. The grid distances and the  
28  
29 time step were studied and chosen to be sufficiently small to get an accurate calculation and full numerical  
30  
31 convergence. All simulations were carried out on an Intel® 3.2 GHz computer with 2.5 GB RAM and  
32  
33 computing times of up to 240 minutes per cyclic-voltammetry simulation were required in order to obtain  
34  
35 a highly accurate two dimensional simulation.

## 36 37 38 39 **Results and Discussion**

40  
41  
42 First, finite potential step chronoamperometry is considered using the ferrocyanide/ferricyanide  
43  
44 ( $[\text{Fe}(\text{CN})_6]^{4-} / [\text{Fe}(\text{CN})_6]^{3-}$ ) redox couple as a model. Experiments were performed at glassy carbon  
45  
46 electrodes of radii of  $1.49 \pm 0.02 \text{ mm}$  and  $0.78 \pm 0.03 \text{ mm}$  employing an aqueous solution of  $9.50 \text{ mM}$   
47  
48  $\text{K}_4[\text{Fe}(\text{CN})_6]$  and  $0.50 \text{ M KNO}_3$  as the electrolyte. Figure 1 shows the current-time transients resulting  
49  
50 from a potential step from  $-0.2 \text{ V vs SCE}$  to  $+0.35 \text{ V vs SCE}$ , corresponding to a potential of zero current  
51  
52 to mass transport limited oxidation of ferrocyanide.

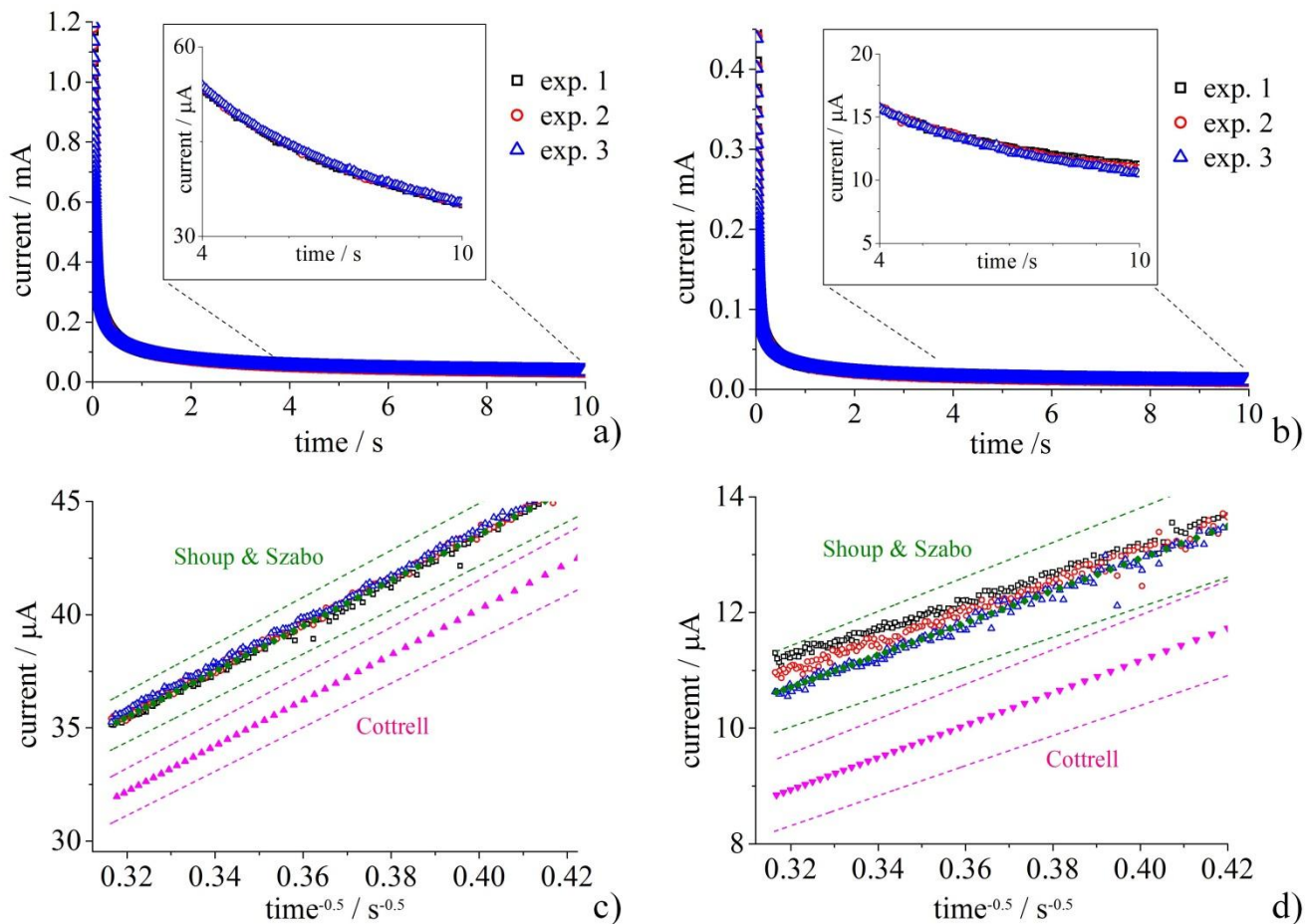


**Figure 1:** Experimental chronoamperograms ( $I-t$ ) recorded for 3 experiments (empty symbols) during the mass transport limited oxidation of  $\text{Fe}(\text{CN})_6]^{4-}$  at millimeter-sized glassy carbon electrodes of a)  $r_e = 1.49$  mm and b)  $r_e = 0.79$  mm and c,d) the comparison of experimental currents (empty symbols) with theoretical currents (solid symbols) as predicted by the Cottrell equation (eq. (1), pink) and the Shoup and Szabo equations (eq. (7)-(9), green); the dashed lines show the respective theoretical currents for maximum experimental variations according to the estimated errors in  $D$  and  $r_e$ ; electrolyte: 9.50 mM  $\text{K}_4\text{Fe}(\text{CN})_6$ , 0.5 M  $\text{KNO}_3$ , potentiostated at  $E = 0.35$  V vs SCE, time step for current measurement: 0.001 s, temperature =  $26.0 \pm 0.2$  °C.

In order to fit the experimental data to the Cottrell equation (equation 1), it is necessary to know the electrode size and the diffusion coefficient of  $\text{Fe}(\text{CN})_6]^{4-}$  in the electrolyte at the experimental temperature. The former was measured (see Experimental) by optical microscopy to  $1.49 \pm 0.02$  mm and  $0.78 \pm 0.03$  mm radius for the two electrodes. The diffusion coefficient of  $\text{Fe}(\text{CN})_6]^{4-}$  was measured using a platinum micro electrode (radius  $r_e = 4.8$   $\mu\text{m}$ ) and calculated from the resulting limiting current according to:

$$I_{ss} = 4Fr_eD[A]_{\text{bulk}} \quad (6)$$

for different temperatures in the range of 24 °C to 28 °C. The measured steady-state voltammograms and the Arrhenius diagram derived from this data are plotted in Figs. 2a and 2b. Thus, the diffusion coefficient of  $\text{Fe}(\text{CN})_6^{4-}$  at the used experimental conditions and the error associated with the estimated maximum temperature uncertainties during the chronoamperometric analysis were determined. Note that the obtained value for  $D$  at 25 °C is in agreement with the values reported for similar electrolytes [28] and the temperature dependency yields an activation energy  $E_a$  for diffusion of ca.  $15.7 \pm 0.3 \text{ kJ mol}^{-1}$  ‡, a value close to that expected from the temperature-dependent viscosity of water [29]. Based on this, the value of  $D$  for the experimental temperature of 26 °C for all chronoamperometric measurements was determined to be  $7.68 \pm 0.03 \times 10^{-10} \text{ m}^2 \text{ s}^{-2}$  (estimating an experimental temperature error of  $\pm 0.2 \text{ }^\circ\text{C}$ ).

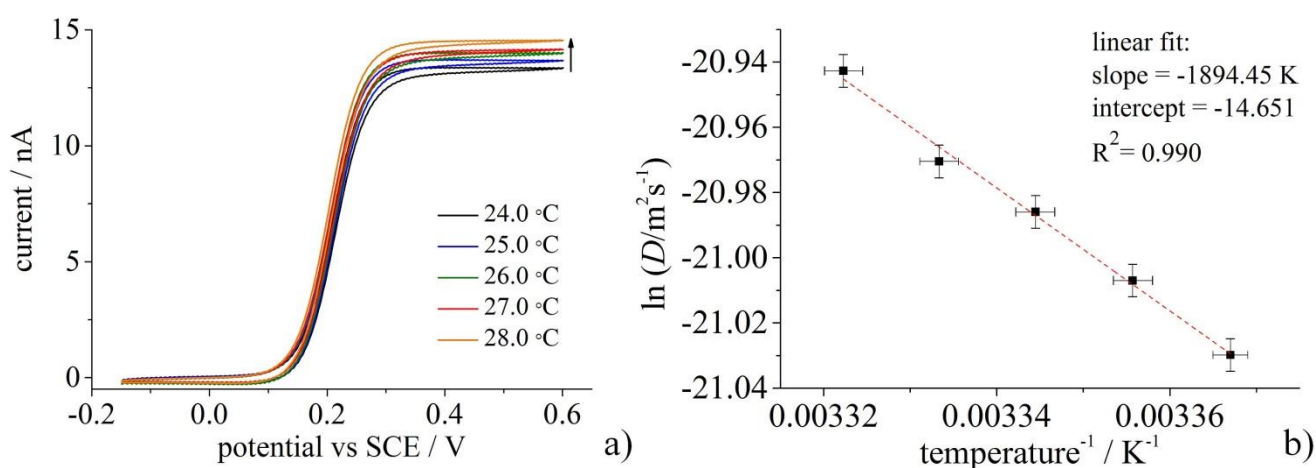


**Figure 2:** a) Steady-state voltammograms at a Pt micro disc electrode ( $r_e = 4.8 \mu\text{m}$ ) recorded at different temperatures. b) Arrhenius plot ( $\ln D$  vs.  $T^{-1}$ ) of the derived diffusion coefficient of  $\text{Fe}(\text{CN})_6^{4-}$  as a function of temperature; the linear fit (dashed line) of the data and the fitted parameters are given in the figure.

The values for the *Cottrellian* current (according to eq. (1), pink triangles) shown in Fig 1c and 1d and the expected error calculated from the possible uncertainties in the electrode size and diffusion coefficient (pink dashed lines) reveal that over the time scale from 0 to 10 seconds the experimental currents are clearly larger than predicted. The difference between the predicted and the observed current is greater for the smaller electrode (Fig. 1d) than for the larger one (Fig. 1c). Natural convection is not thought to play a dominant role at the timescale of interest ( $\leq 10$  seconds), so the additional contribution of radial diffusion was considered as a plausible explanation for the augmented currents observed. Potential step chronoamperometry under these conditions has been extensively simulated and a particularly reliable calculation was reported by Shoup and Szabo [30]. The accuracy of their approach has been confirmed by

‡ The Arrhenius relation is  $\ln D = \text{constant} - E_a R^{-1} T^{-1}$ , hence, the slope of the linear fit shown in Fig. 2b provides the activation energy for the diffusion of  $\text{Fe}(\text{CN})_6^{4-}$  in the electrolyte upon multiplication by  $-R$ .

1  
2  
3 many works[31–34]. For instance Klymenko, Svir et al. [35] presented their simulations on the basis of  
4 the *Shoup and Szabo* equations, which have been found well-suited for the analysis of experimental data  
5 [36, 37].  
6  
7

$$9 \quad I = 4FDr_e[A]_{\text{bulk}} f(\tau) \quad (7)$$

10 where the dimensionless time  $\tau$  is defined as  
11  
12

$$13 \quad \tau = 4Dtr_e^{-2} \quad (8)$$

14  
15 For short dimensionless times ( $\tau < 1$ )  $f(\tau)$  can be approximated as  
16  
17

$$18 \quad f(\tau) = \left(\frac{\pi}{4\tau}\right)^{0.5} + \frac{\pi}{4} + 0.094\tau^{0.5} \quad (9)$$

19  
20 and for long times ( $\tau > 1$ )  
21  
22

$$23 \quad f(\tau) = 1 + 0.71835\tau^{-0.5} + 0.05626\tau^{-1.5} - 0.00646\tau^{-2.5} \quad (10)$$

24  
25 The use of equations (7-9) to appropriately model the data presented in Fig. 1a and 1b suggests that the  
26 observed deviation from the purely Cottrellian behaviour can be attributed to radial diffusion effects.  
27  
28 Figure 1c and 1d show the excellent agreement between experiment and theory, validating that diffusion-  
29 only mass transport conditions were achieved in the experiment. It follows that electrodes of 0.78 mm and  
30 1.49 mm radius are *not* sufficiently large to ensure pure one-dimensional diffusion over a time scale of  
31 several seconds. Note that such electrode dimensions are typical sizes of many commercially supplied  
32 ‘macro’ electrodes.  
33  
34

35  
36 Given the significant contribution of radial diffusion to chronoamperometric currents at millimetre-sized  
37 electrodes, the effect of these contributions on cyclic voltammetry will be considered and quantified using  
38 simulations in the following section.  
39  
40

41  
42 For this purpose the above-mentioned A/B redox couple was assumed to be fully electrochemically  
43 reversible and Nernst boundary conditions were applied to predict the current. Voltammetric curves in the  
44 presence and absence of radial diffusion were simulated and validated by comparison with analytical  
45 theory [27]. Figure 3 depicts the simulated voltammograms.  
46  
47  
48  
49  
50  
51  
52  
53  
54  
55  
56  
57  
58  
59  
60  
61  
62  
63  
64  
65

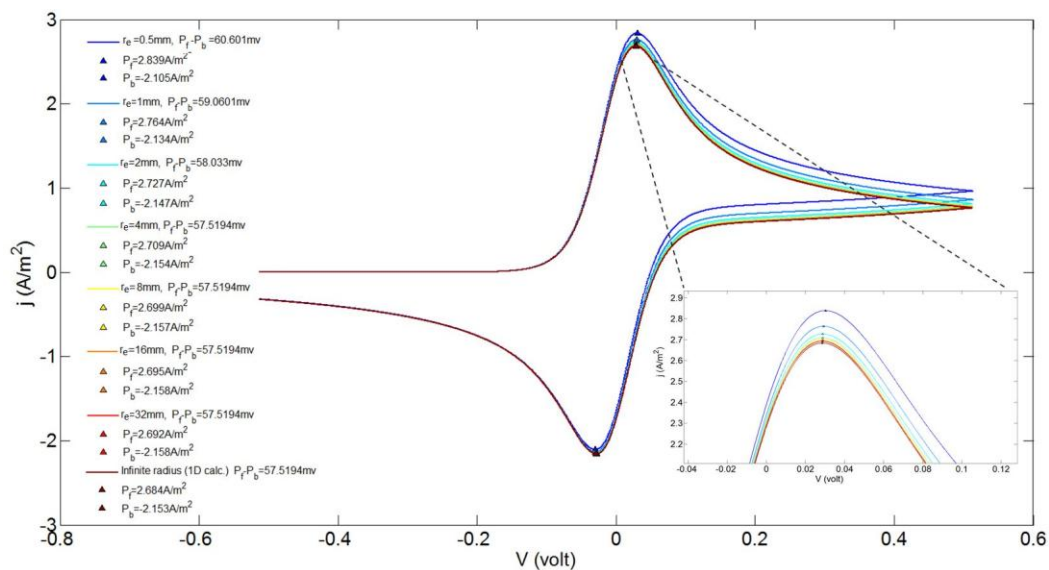


**Figure 3:** Voltammograms simulated assuming an electrochemically reversible redox couple A/B with Nernst boundary conditions and diffusion coefficients of  $D_A = D_B = 1 \times 10^{-9} \text{ m}^2 \text{ s}^{-2}$ . Voltammetric currents for various electrode sizes (radius =  $r_e$ ) are normalized by the area ( $A = \pi r_e^2$ ) of the macro disc working electrode and the resulting current densities ( $j$ ) are shown. The inset provides an enlarged view of the oxidative forward peak ( $P_f$ ) current densities ( $j_p$ ).

A visible – and experimentally measurable – difference between the behaviour calculated using planar diffusion only and the full simulation of the finite electrode size is apparent. The ‘reversibility’ of redox couples is generally measured via the peak-to-peak voltage separation  $E_{pp}$ . Table 1 summarises the variations of the peak current density  $j_p$  and  $E_{pp}$  values for different electrode sizes and scan rates, taking all other parameters as given in Figure 3. It is again evident that the electrodes of size of ca. 1 mm radius show significant deviations from the simple one-dimensional diffusion limit. Note that experimental observations of this kind in experiments could easily be miss-interpreted as electrode kinetics rather than geometric, mass transport effects.

**Table 1:** Simulated voltammetric peak to peak separations and oxidative peak current densities for ‘macro’ disc electrodes of different radii in comparison to the results expected for a truly one-dimensional planar diffusion to an electrode of infinite size.

electrode radius $r_e$ / mm	Peak-to-peak separation $E_{PP}$ / mV	ox. peak current density $j_P$ / $\text{Am}^{-2}$
0.5	60.60	2.84
1	59.06	2.76
2	58.0	2.73
4	57.52	2.71
8	57.52	2.70
16	57.52	2.69
32	57.52	2.69
infinite (1D calc.)	57.52	2.68

## Conclusions

If quantitative measurements are to be made in which experiments are coupled with theory then macro electrodes need to be selected with multi-millimeter radius to avoid contributions of ‘edge effects’ originating from radial contributions. Several commercially available ‘macro’ electrodes are likely to be too small to meet this requirement; rather electrodes of size not less than 4 mm radius are recommended for investigations in aqueous solutions. As diffusion coefficients of redox species are typically larger in organic solvents and smaller in many room temperature ionic liquids, larger and smaller minimum electrode sizes are required for a true ‘macro’ response in these cases, respectively. Alternatively, the use of microelectrodes may be preferred, especially for electro kinetic measurements.

## Acknowledgements

KT was supported by a Marie Curie Intra European Fellowship (Grant Agreement no. [327706]) within the 7th European Community Framework Programme. SE and RGC acknowledge funding from the European Research Council under the European Union's Seventh Framework Programme (FP/2007-2013) / ERC Grant Agreement no. [320403].

1  
2  
3  
4  
5  
6  
7  
8 **References**  
9

- 10  
11 1. Amatore CA, Deakin MR, Wightman M (1986) Electrochemical kinetics at microelectrodes Part 1.  
12 Quasi-reversible electron transfer at cylinders. *J Electroanal Chem Interfacial Electrochem* 206:23–36.  
13 doi: 10.1016/0022-0728(86)90253-6  
14  
15  
16  
17 2. Amatore C, Deakin MR, Wightman RM (1987) Electrochemical kinetics at microelectrodes: Part IV.  
18 Electrochemistry in media of low ionic strength. *J Electroanal Chem Interfacial Electrochem* 225:49–  
19 63. doi: 10.1016/0022-0728(87)80004-9  
20  
21  
22  
23 3. Bond AM, Oldham KB, Zoski CG (1988) Theory of electrochemical processes at an inlaid disc  
24 microelectrode under steady-state conditions. *J Electroanal Chem Interfacial Electrochem* 245:71–104.  
25 doi: 10.1016/0022-0728(88)80060-3  
26  
27  
28  
29 4. Bond AM (1994) Past, present and future contributions of microelectrodes to analytical studies  
30 employing voltammetric detection. A review. *Analyst* 119:1R–21R. doi: 10.1039/AN994190001R  
31  
32  
33  
34 5. Scholz F (2009) *Electroanalytical Methods: Guide to Experiments and Applications*. Springer Science  
35 & Business Media  
36  
37  
38  
39 6. Montenegro MI, Montenegro I, Queirós MA, Daschbach JL (1991) *Microelectrodes: Theory and*  
40 *Applications: Theory and Applications*. Springer Science & Business Media  
41  
42  
43  
44 7. Mayrhofer KJJ, Strmcnik D, Blizanac BB, et al. (2008) Measurement of oxygen reduction activities via  
45 the rotating disc electrode method: From Pt model surfaces to carbon-supported high surface area  
46 catalysts. *Electrochimica Acta* 53:3181–3188. doi: 10.1016/j.electacta.2007.11.057  
47  
48  
49  
50 8. Concepcion JJ, Binstead RA, Alibabaei L, Meyer TJ (2013) Application of the Rotating Ring-Disc-  
51 Electrode Technique to Water Oxidation by Surface-Bound Molecular Catalysts. *Inorg Chem*  
52 52:10744–10746. doi: 10.1021/ic402240t  
53  
54  
55  
56  
57  
58  
59  
60  
61  
62  
63  
64  
65

- 1  
2  
3 9. Simonov AN, Kemppinen P, Pozo-Gonzalo C, et al. (2014) Aggregation of a Dibenzo[b,def]chrysene  
4 Based Organic Photovoltaic Material in Solution. *J Phys Chem B* 118:6839–6849. doi:  
5 10.1021/jp501220v  
6  
7  
8  
9  
10 10. Nicholson RS, Shain I (1964) Theory of Stationary Electrode Polarography. Single Scan and Cyclic  
11 Methods Applied to Reversible, Irreversible, and Kinetic Systems. *Anal Chem* 36:706–723. doi:  
12 10.1021/ac60210a007  
13  
14  
15  
16 11. Nicholson RS, Shain I (1965) Theory of Stationary Electrode Polarography for a Chemical Reaction  
17 Coupled between Two Charge Transfers. *Anal Chem* 37:178–190. doi: 10.1021/ac60221a002  
18  
19  
20  
21 12. Cottrell FG (1902) *Z Für Phys Chem* 42:385.  
22  
23  
24 13. Compton RG, Banks CE (2011) *Understanding Voltammetry*, 2nd ed. World Scientific  
25  
26  
27 14. Fick A (1855) Ueber Diffusion. *Ann Phys* 170:59–86. doi: 10.1002/andp.18551700105  
28  
29  
30 15. Fick A (1855) V. On liquid diffusion. *Philos Mag Ser 4* 10:30–39. doi: 10.1080/14786445508641925  
31  
32  
33 16. Morris GP, Simonov AN, Mashkina EA, et al. (2013) A Comparison of Fully Automated Methods of  
34 Data Analysis and Computer Assisted Heuristic Methods in an Electrode Kinetic Study of the  
35 Pathologically Variable [Fe(CN)<sub>6</sub>]<sup>3-/4-</sup> Process by AC Voltammetry. *Anal Chem* 85:11780–11787.  
36 doi: 10.1021/ac4022105  
37  
38  
39  
40 17. Bentley CL, Bond AM, Hollenkamp AF, et al. (2014) Applications of Convolution Voltammetry in  
41 Electroanalytical Chemistry. *Anal Chem* 86:2073–2081. doi: 10.1021/ac4036422  
42  
43  
44  
45 18. Simonov AN, Morris GP, Mashkina EA, et al. (2014) Inappropriate Use of the Quasi-Reversible  
46 Electrode Kinetic Model in Simulation-Experiment Comparisons of Voltammetric Processes That  
47 Approach the Reversible Limit. *Anal Chem* 86:8408–8417. doi: 10.1021/ac5019952  
48  
49  
50  
51 19. Norouzi P, Ganjali MR, Daneshgar P, Mohammadi A (2007) Fast Fourier Transform Continuous  
52 Cyclic Voltammetry Development as a Highly Sensitive Detection System for Ultra Trace Monitoring  
53 of Thiamine. *Anal Lett* 40:547–559. doi: 10.1080/00032710600964874  
54  
55  
56  
57  
58  
59  
60  
61  
62  
63  
64  
65

- 1  
2  
3 20. Ebrahimi B, Shojaosadati SA, Daneshgar P, et al. (2011) Performance evaluation of fast Fourier-  
4 transform continuous cyclic-voltammetry pesticide biosensor. *Anal Chim Acta* 687:168–176. doi:  
5 10.1016/j.aca.2010.12.005  
6  
7  
8  
9 21. Amatore C, Pebay C, Thouin L, et al. (2010) Difference between Ultramicroelectrodes and  
10 Microelectrodes: Influence of Natural Convection. *Anal Chem* 82:6933–6939. doi:  
11 10.1021/ac101210r  
12  
13  
14  
15 22. Amatore C, Klymenko OV, Svir I (2012) Importance of Correct Prediction of Initial Concentrations in  
16 Voltammetric Scans: Contrasting Roles of Thermodynamics, Kinetics, and Natural Convection. *Anal*  
17 *Chem* 84:2792–2798. doi: 10.1021/ac203188b  
18  
19  
20  
21 23. Barnes AS, Streeter I, Compton RG (2008) On the use of digital staircase ramps for linear sweep  
22 voltammetry at microdisc electrodes: Large step potentials significantly broaden and shift  
23 voltammetric peaks. *J Electroanal Chem* 623:129–133. doi: 10.1016/j.jelechem.2008.06.022  
24  
25  
26  
27  
28 24. Ward KR, Compton RG (2014) Quantifying the apparent “Catalytic” effect of porous electrode  
29 surfaces. *J Electroanal Chem* 724:43–47. doi: 10.1016/j.jelechem.2014.04.009  
30  
31  
32  
33 25. Ward KR, Gara M, Lawrence NS, et al. (2013) Nanoparticle modified electrodes can show an  
34 apparent increase in electrode kinetics due solely to altered surface geometry: The effective  
35 electrochemical rate constant for non-flat and non-uniform electrode surfaces. *J Electroanal Chem*  
36 695:1–9. doi: 10.1016/j.jelechem.2013.02.012  
37  
38  
39  
40  
41 26. Compton RG, Laborda E, Ward KR (2013) *Understanding Voltammetry: Simulation of Electrode*  
42 *Processes*. Imperial College Press, London  
43  
44  
45  
46 27. Eloul S, Compton RG (2014) Shielding of a Microdisc Electrode Surrounded by an Adsorbing  
47 Surface. *ChemElectroChem* 1:917–924. doi: 10.1002/celec.201400005  
48  
49  
50  
51 28. Konopka SJ, McDuffie B (1970) Diffusion coefficients of ferri- and ferrocyanide ions in aqueous  
52 media, using twin-electrode thin-layer electrochemistry. *Anal Chem* 42:1741–1746. doi:  
53 10.1021/ac50160a042  
54  
55  
56  
57 29. Lide DR (2008) *CRC handbook of Chemistry and Physics*, 89th ed. Taylor & Francis Group  
58  
59  
60  
61  
62  
63  
64  
65

- 1  
2  
3 30. Shoup D, Szabo A (1982) Chronoamperometric current at finite disk electrodes. *J Electroanal Chem*  
4 *Interfacial Electrochem* 140:237–245. doi: 10.1016/0022-0728(82)85171-1  
5  
6  
7  
8 31. Heinze J (1981) Diffusion processes at finite (micro) disk electrodes solved by digital simulation. *J*  
9 *Electroanal Chem Interfacial Electrochem* 124:73–86. doi: 10.1016/S0022-0728(81)80285-9  
10  
11  
12 32. Heinze J, Storzbach M (1991) Digital Simulation of Mass Transport to Ultramicroelectrodes.  
13 *Conference Proceeding NATO Advanced Study Inst on Microelectrodes: Theory and Applications*  
14  
15  
16  
17 33. Britz D, Oldham KB, Østerby O (2009) Strategies for damping the oscillations of the alternating  
18 direction implicit method of simulation of diffusion-limited chronoamperometry at disk electrodes.  
19 *Electrochimica Acta* 54:4822–4828. doi: 10.1016/j.electacta.2009.03.087  
20  
21  
22  
23 34. Britz D, Østerby O, Strutwolf J (2012) Minimum grid digital simulation of chronoamperometry at a  
24 disk electrode. *Electrochimica Acta* 78:365–376. doi: 10.1016/j.electacta.2012.06.009  
25  
26  
27  
28 35. Klymenko OV, Evans RG, Hardacre C, et al. (2004) Double potential step chronoamperometry at  
29 microdisk electrodes: simulating the case of unequal diffusion coefficients. *J Electroanal Chem*  
30 *571:211–221*. doi: 10.1016/j.jelechem.2004.05.012  
31  
32  
33  
34 36. Xiong L, Aldous L, Henstridge MC, Compton RG (2012) Investigation of the optimal transient times  
35 for chronoamperometric analysis of diffusion coefficients and concentrations in non-aqueous solvents  
36 and ionic liquids. *Anal Methods* 4:371. doi: 10.1039/c1ay05667k  
37  
38  
39  
40  
41 37. Paddon CA, Bhatti FL, Donohoe TJ, Compton RG (2006) Cryo-electrochemistry in tetrahydrofuran:  
42 The electrochemical reduction of a phenyl thioether: [(3-{{trans-4-  
43 (Methoxymethoxy)cyclohexyl}oxy}propyl)thio]benzene. *J Electroanal Chem* 589:187–194. doi:  
44 10.1016/j.jelechem.2006.02.010  
45  
46  
47  
48  
49  
50  
51  
52  
53  
54  
55  
56  
57  
58  
59  
60  
61  
62  
63  
64  
65

1  
2  
3  
4  
5  
6  
7  
8  
9  
10  
11  
12  
13  
14  
15  
16  
17  
18  
19  
20  
21  
22  
23  
24  
25  
26  
27  
28  
29  
30  
31  
32  
33  
34  
35  
36  
37  
38  
39  
40  
41  
42  
43  
44  
45  
46  
47  
48  
49  
50  
51  
52  
53  
54  
55  
56  
57  
58  
59  
60  
61  
62  
63  
64  
65

## References

1. Amatore CA, Deakin MR, Wightman M (1986) Electrochemical kinetics at microelectrodes Part 1. Quasi-reversible electron transfer at cylinders. *J Electroanal Chem Interfacial Electrochem* 206:23–36
2. Amatore C, Deakin MR, Wightman RM (1987) Electrochemical kinetics at microelectrodes: Part IV. Electrochemistry in media of low ionic strength. *J Electroanal Chem Interfacial Electrochem* 225:49–63
3. Bond AM, Oldham KB, Zoski CG (1988) Theory of electrochemical processes at an inlaid disc microelectrode under steady-state conditions. *J Electroanal Chem Interfacial Electrochem* 245:71–104
4. Bond AM (1994) Past, present and future contributions of microelectrodes to analytical studies employing voltammetric detection. A review. *Analyst* 119:1R–21R
5. Scholz F (2009) *Electroanalytical Methods: Guide to Experiments and Applications*. Springer Science & Business Media
6. Montenegro MI, Montenegro I, Queirós MA, Daschbach JL (1991) *Microelectrodes: Theory and Applications: Theory and Applications*. Springer Science & Business Media
7. Mayrhofer KJJ, Strmcnik D, Blizanac BB, et al. (2008) Measurement of oxygen reduction activities via the rotating disc electrode method: From Pt model surfaces to carbon-supported high surface area catalysts. *Electrochimica Acta* 53:3181–3188
8. Concepcion JJ, Binstead RA, Alibabaei L, Meyer TJ (2013) Application of the Rotating Ring-Disc-Electrode Technique to Water Oxidation by Surface-Bound Molecular Catalysts. *Inorg Chem* 52:10744–10746
9. Simonov AN, Kempainen P, Pozo-Gonzalo C, et al. (2014) Aggregation of a Dibenzo[b,def]chrysene Based Organic Photovoltaic Material in Solution. *J Phys Chem B* 118:6839–6849
10. Nicholson RS, Shain I (1964) Theory of Stationary Electrode Polarography. Single Scan and Cyclic Methods Applied to Reversible, Irreversible, and Kinetic Systems. *Anal Chem* 36:706–723

- 1  
2  
3 11. Nicholson RS, Shain I (1965) Theory of Stationary Electrode Polarography for a Chemical Reaction  
4 Coupled between Two Charge Transfers. *Anal Chem* 37:178–190  
5  
6
- 7  
8 12. Cottrell FG (1902) *Z Für Phys Chem* 42:385  
9
- 10  
11 13. Compton RG, Banks CE (2011) *Understanding Voltammetry*, 2nd ed. World Scientific  
12
- 13  
14 14. Fick A (1855) Ueber Diffusion. *Ann Phys* 170:59–86  
15
- 16  
17 15. Fick A (1855) V. On liquid diffusion. *Philos Mag Ser 4* 10:30–39  
18
- 19  
20 16. Morris GP, Simonov AN, Mashkina EA, et al. (2013) A Comparison of Fully Automated Methods of  
21 Data Analysis and Computer Assisted Heuristic Methods in an Electrode Kinetic Study of the  
22 Pathologically Variable  $[\text{Fe}(\text{CN})_6]^{3-/4-}$  Process by AC Voltammetry. *Anal Chem* 85:11780–11787  
23  
24
- 25  
26 17. Bentley CL, Bond AM, Hollenkamp AF, et al. (2014) Applications of Convolution Voltammetry in  
27 Electroanalytical Chemistry. *Anal Chem* 86:2073–2081  
28  
29
- 30  
31 18. Simonov AN, Morris GP, Mashkina EA, et al. (2014) Inappropriate Use of the Quasi-Reversible  
32 Electrode Kinetic Model in Simulation-Experiment Comparisons of Voltammetric Processes That  
33 Approach the Reversible Limit. *Anal Chem* 86:8408–8417  
34  
35  
36
- 37  
38 19. Norouzi P, Ganjali MR, Daneshgar P, Mohammadi A (2007) Fast Fourier Transform Continuous  
39 Cyclic Voltammetry Development as a Highly Sensitive Detection System for Ultra Trace Monitoring  
40 of Thiamine. *Anal Lett* 40:547–559  
41  
42
- 43  
44 20. Ebrahimi B, Shojaosadati SA, Daneshgar P, et al. (2011) Performance evaluation of fast Fourier-  
45 transform continuous cyclic-voltammetry pesticide biosensor. *Anal Chim Acta* 687:168–176  
46  
47
- 48  
49 21. Amatore C, Pebay C, Thouin L, et al. (2010) Difference between Ultramicroelectrodes and  
50 Microelectrodes: Influence of Natural Convection. *Anal Chem* 82:6933–6939  
51  
52
- 53  
54 22. Amatore C, Klymenko OV, Svir I (2012) Importance of Correct Prediction of Initial Concentrations in  
55 Voltammetric Scans: Contrasting Roles of Thermodynamics, Kinetics, and Natural Convection. *Anal*  
56 *Chem* 84:2792–2798  
57  
58  
59  
60  
61  
62  
63  
64  
65

- 1  
2  
3 23. Barnes AS, Streeter I, Compton RG (2008) On the use of digital staircase ramps for linear sweep  
4 voltammetry at microdisc electrodes: Large step potentials significantly broaden and shift  
5 voltammetric peaks. *J Electroanal Chem* 623:129–133  
6  
7  
8  
9 24. Ward KR, Compton RG (2014) Quantifying the apparent “Catalytic” effect of porous electrode  
10 surfaces. *J Electroanal Chem* 724:43–47  
11  
12  
13  
14 25. Ward KR, Gara M, Lawrence NS, et al. (2013) Nanoparticle modified electrodes can show an  
15 apparent increase in electrode kinetics due solely to altered surface geometry: The effective  
16 electrochemical rate constant for non-flat and non-uniform electrode surfaces. *J Electroanal Chem*  
17 695:1–9  
18  
19  
20  
21  
22 26. Compton RG, Laborda E, Ward KR (2013) *Understanding Voltammetry: Simulation of Electrode*  
23 *Processes*. Imperial College Press, London  
24  
25  
26  
27 27. Eloul S, Compton RG (2014) Shielding of a Microdisc Electrode Surrounded by an Adsorbing  
28 Surface. *ChemElectroChem* 1:917–924  
29  
30  
31  
32 28. Konopka SJ, McDuffie B (1970) Diffusion coefficients of ferri- and ferrocyanide ions in aqueous  
33 media, using twin-electrode thin-layer electrochemistry. *Anal Chem* 42:1741–1746  
34  
35  
36  
37 29. Lide DR (2008) *CRC handbook of Chemistry and Physics*, 89th ed. Taylor & Francis Group  
38  
39  
40 30. Shoup D, Szabo A (1982) Chronoamperometric current at finite disk electrodes. *J Electroanal Chem*  
41 *Interfacial Electrochem* 140:237–245  
42  
43  
44 31. Heinze J (1981) Diffusion processes at finite (micro) disk electrodes solved by digital simulation. *J*  
45 *Electroanal Chem Interfacial Electrochem* 124:73–86  
46  
47  
48  
49 32. Heinze J, Storzbach M (1991) Digital Simulation of Mass Transport to Ultramicroelectrodes.  
50 *Conference Proceeding NATO Advanced Study Inst on Microelectrodes: Theory and Applications*  
51  
52  
53  
54 33. Britz D, Oldham KB, Østerby O (2009) Strategies for damping the oscillations of the alternating  
55 direction implicit method of simulation of diffusion-limited chronoamperometry at disk electrodes.  
56 *Electrochimica Acta* 54:4822–4828  
57  
58  
59  
60  
61  
62  
63  
64  
65

- 1  
2  
3 34. Britz D, Østerby O, Strutwolf J (2012) Minimum grid digital simulation of chronoamperometry at a  
4 disk electrode. *Electrochimica Acta* 78:365–376  
5  
6  
7  
8 35. Klymenko OV, Evans RG, Hardacre C, et al. (2004) Double potential step chronoamperometry at  
9 microdisk electrodes: simulating the case of unequal diffusion coefficients. *J Electroanal Chem*  
10 571:211–221  
11  
12  
13  
14 36. Xiong L, Aldous L, Henstridge MC, Compton RG (2012) Investigation of the optimal transient times  
15 for chronoamperometric analysis of diffusion coefficients and concentrations in non-aqueous solvents  
16 and ionic liquids. *Anal Methods* 4:371  
17  
18  
19  
20  
21 37. Paddon CA, Bhatti FL, Donohoe TJ, Compton RG (2006) Cryo-electrochemistry in tetrahydrofuran:  
22 The electrochemical reduction of a phenyl thioether: [(3-{{trans-4-  
23 (Methoxymethoxy)cyclohexyl}oxy}propyl)thio]benzene. *J Electroanal Chem* 589:187–194.  
24  
25  
26  
27  
28  
29  
30  
31  
32  
33  
34  
35  
36  
37  
38  
39  
40  
41  
42  
43  
44  
45  
46  
47  
48  
49  
50  
51  
52  
53  
54  
55  
56  
57  
58  
59  
60  
61  
62  
63  
64  
65